

## Recent Results from the Tokyo-EBIT

Shunsuke Ohtani

*“Cold Trapped Ions” Project, ICORP, JST and The University of Electro-Communications,  
Chofu, 182-8585 Tokyo, Japan*

A number of different experiments are progressing in parallel for the study of the physics of highly charged ions using the Tokyo-EBIT. This paper gives the general feature of the apparatus and surveys some recent works performed with it.

### INTRODUCTION

The electron beam ion trap (EBIT) is a unique ion source as a means of producing and trapping highly charged ions (HCIs). It was developed at the Lawrence Livermore National Laboratory initially for spectroscopic studies,<sup>1</sup> which was based on the earlier electron beam ion source (EBIS) concepts<sup>2</sup> but with a shorter ion-trap length to limit plasma-like instabilities and hence to increase the residence time of trapped ions. The long residence time is essentially important for producing the higher charge-state ions and observing them in spectroscopic studies.

Several EBITs have been constructed throughout the world. Most EBITs have similar operation parameters with an electron beam energy of up to 25 keV. For highly stripped ions of heavy atoms (high-Z elements), the ionization cross sections by electron impact increase gradually with the electron energy. Therefore a high energy electron beam is favorable for producing high-Z ions with very high-charge states. In Livermore, a high-energy EBIT is in operation presently to perform the spectroscopic studies for systematic investigation of the relativistic and QED effects in simple atomic systems. A new high-energy EBIT is under development in Freiburg to perform atomic collision experiments with extracted HCIs as well as spectroscopy.<sup>3</sup>

A few years ago, we have also constructed a newly designed, high-energy EBIT in Tokyo to develop a new research field in atomic physics with HCIs.<sup>4</sup> In the first stage of the operation, our experimental activity has been concentrated mainly on the spectroscopy of HCIs in the trap. Recently, we have started to use the extracted ions from the trap and to investigate the HCI-interaction with matter.

In this report, an overview of the Tokyo-EBIT and some recent results with it are shown.

### DESIGN AND OPERATION

In general, the EBIT device consists of three parts: an electron gun, a trap region with three drift tubes and an electron collector. A schematic view of the Tokyo-EBIT and the ion trap region are shown in Fig. 1. The electron beam emitted from the gun is accelerated upwards by the potential difference between the gun and the drift tubes, whilst being compressed to a radius of about 30  $\mu\text{m}$  by a 4.5 T magnetic field generated by superconducting Helmholtz coils. After passing through the drift tubes, the electrons are decelerated and collected by the electron collector. Both the electron gun and the collector are designed to be floated to max. -300 kV.

Neutrals or ions are injected into the trap through a gas valve or from a pulsed ion source of vacuum-spark-type. Through interaction with the high current-density electron beam, they are ionized successively in the trap region. Ions produced are trapped radially by the space charge potential ( $\sim 10$  V) of the electron beam and axially by voltages ( $\sim 100$  V) applied to the drift tubes. The electron beam also serves to excite the trapped ions. Radiation from the excited ions can be observed through radial ports on the center drift tube in the horizontal plane.

The EBIT has several advantages for spectroscopic studies. The ions are nearly at rest, so Doppler shift corrections are not required. The EBIT forms a line light source, that is, the source size is approximately defined by the electron beam radius, so this source can be used directly for dispersive spectroscopy without the need for an entrance slit. The EBIT source is a low-density, low-collisional, weak-field non-neutral plasma, so the absorption of emission lines is negligible and the population of metastable states is also negligible. In addition, because the charge-state distribution in the trap is simple, and subsequently the spectral structure

observed is also simple compared with other plasma sources, the identification of the transition and the measurement of the wavelength can be easily performed.

Fig. 2 shows an X-ray spectrum measured with a Ge solid state detector.

The electron beam parameter in this observation is 75 keV, 150 mA. Krypton gas is introduced into the trap. In the X-ray energy region below the electron beam energy  $E_e$ , a series of K-X-ray lines from highly charged ions of Kr, Ba and W are observed. The Ba and W atoms are evaporated from the cathode, subsequently ionized and trapped. The bremsstrahlung radiation continues up to the beam energy  $E_e$ . Radiative recombination (RR) lines of highly charged ions are also observed in the higher X-ray energy region. RR lines appear at energies above the  $E_e$ , as clearly seen in the expanded X-ray spectrum of the lower figure, since the energy of an RR line is the sum of the  $E_e$  and the ionization energy of the captured electron. The lines observed here are RR to the  $n = 1, 2$  and 3 levels of Kr, Ba and W ions, converging to the  $E_e$ . RR lines to  $n = 1$  level split into two peaks for Ba and Kr ions. The peak at the higher energy side is due to RR into bare ions, and that at the lower side is due to RR into H-like ions. This spectrum shows the production of bare Ba ions ( $Ba^{56+}$ ) in the trap. For Ba, the peak for RR into bare ions is smaller than that for RR

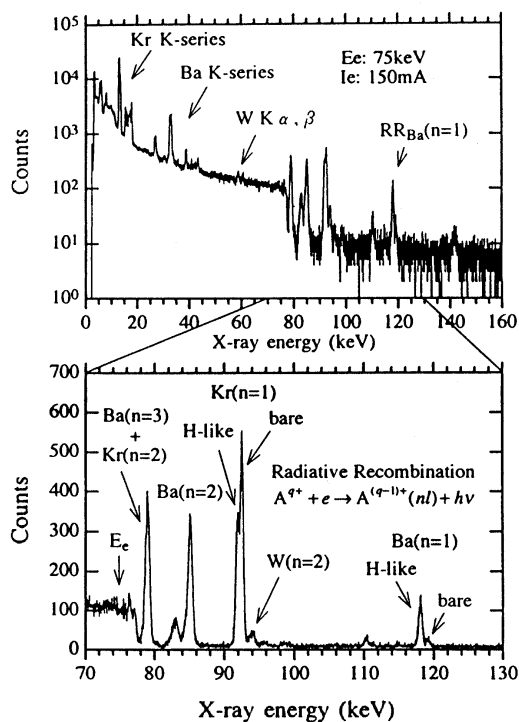


Fig. 2. An X-ray spectrum from the trapped ions observed with a Ge solid state detector.

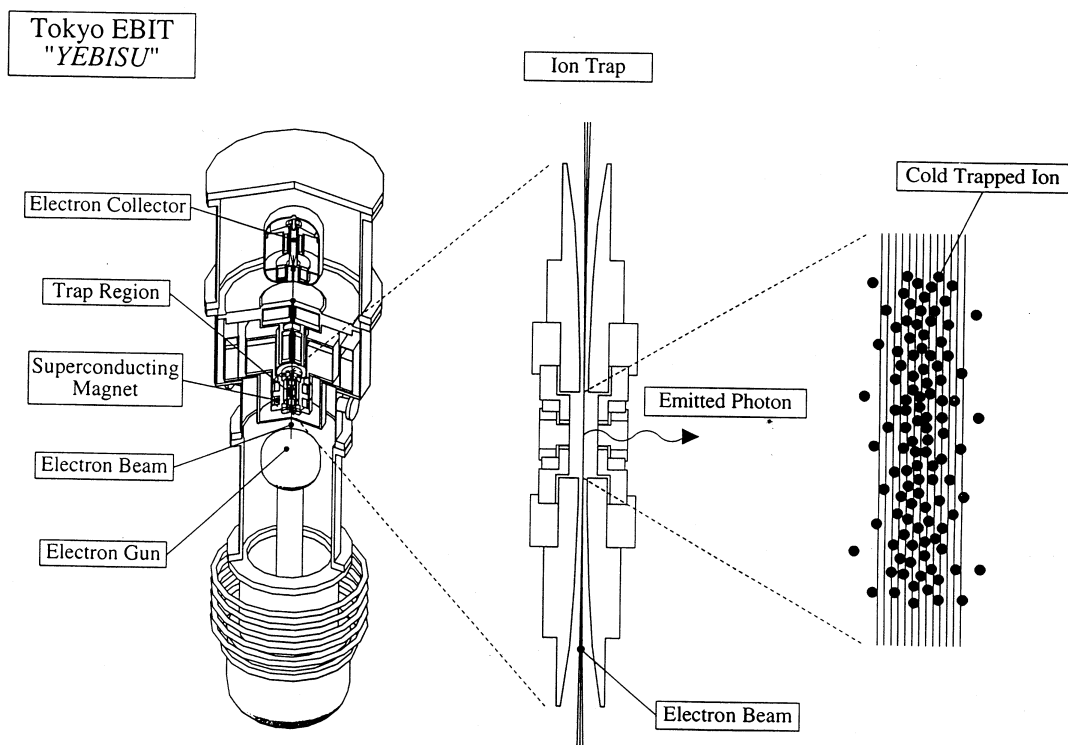


Fig. 1. Schematic view of the Tokyo-EBIT (nick named YEBISU), and the ion-trap region.

into H-like ions, while for Kr the situation is reversed. This implies that the bare  $\text{Kr}^{36+}$  ions are dominantly produced and confined in the trap at this EBIT operation.

The Tokyo-EBIT has a beam transport line for extraction of trapped ions to facilitate HCI-surface and-molecule collision experiments. There are two types of extraction methods: leaky and pulsed mode. Fig. 3 shows typical charge-state distributions for highly charged Kr ions extracted at different operation conditions. The intensity distribution of extracted Kr ions is shown in Fig. 3(a) with the leaky mode for the beam condition of 25 keV, 100 mA.

In the EBIT, trapping efficiency is considered to be

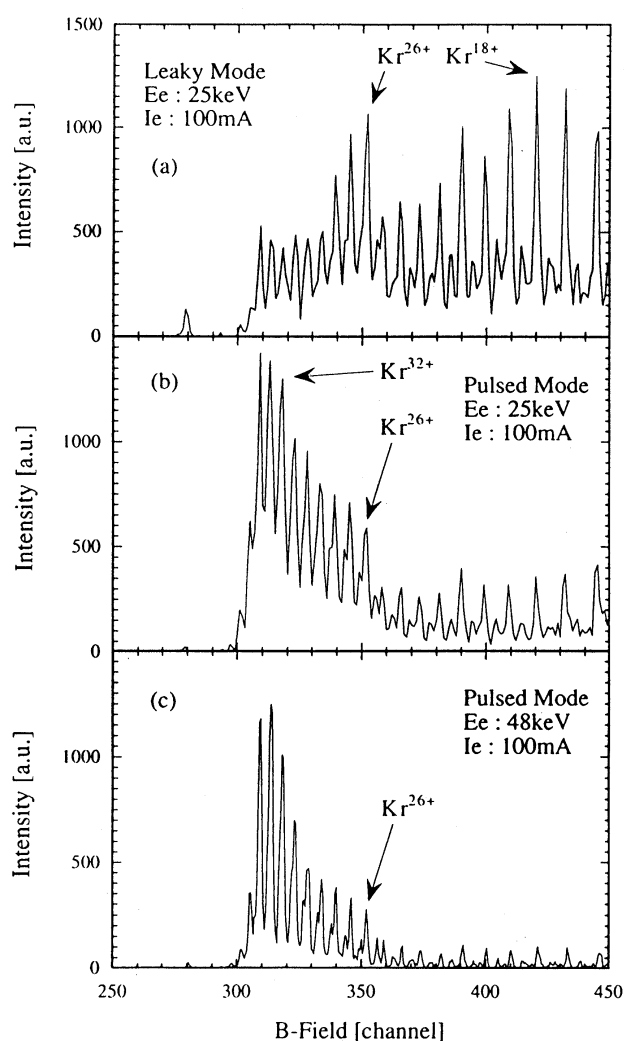


Fig. 3. A charge-state spectrum of Kr ions. The spectrum was obtained using two different extraction modes, (a) leaky mode and (b) (c) pulsed mode.  $E_e$  and  $I_e$  represent the electron energy and the current, respectively, at which the spectra were obtained.

roughly proportional to the charge-state of trapped ions. Therefore, as seen in Fig. 3(a), ions with lower charge-states escape out of the trap easier than the higher charge-state ions. Typical intensity of extracted Ne-like ions ( $\text{Kr}^{26+}$ ) is  $10^4$ - $10^5$  ions per second at the leaky mode. In Fig. 3(b) and 3(c), the charge-state spectra are shown with the pulsed mode at different energies of the electron beam. In the pulsed mode, higher charge-state ions which are efficiently confined in the trap are forced out of the trap by raising the potential applied to the center drift tube, resulting in a larger population of those ions in the spectra. As seen in Fig. 3(b) and 3(c), the relative population of higher charged ions becomes larger at the higher beam-energy operation. The number of extracted ions e.g.  $\text{Kr}^{32+}$  are typically  $10^4$  ions per pulse duration of  $\sim 10$  ms.

## SOME RECENT RESULTS

### X-ray Spectroscopy

In the course of the spectroscopic studies in Tokyo, various kinds of X-ray spectroscopy have been performed, such as the precise measurements of the wavelengths for X-ray transitions, the observation of dielectronic recombination (DR) processes, and the measurements of collision strengths and polarizations as a function of the beam energy in electron-HCI interactions.

In this report, we just show recent systematic measurements of the wavelengths for X-ray transitions in Ne-like, high-Z ions.<sup>5</sup> Because of high abundance in a hot plasma due to its closed shell structure, the investigation of X-ray transitions in the Ne-like sequence is important for applications such as plasma diagnostics and X-ray lasers. From the viewpoint of atomic physics, the systematic study for Ne-like ions is also important to understand the relativistic atomic structure since there is strong configuration mixing of the wave functions of the excited states in the high-Z region.

In the present observation, the spectrometer used consists of a flat LiF(200) crystal with a high-pressure, position-sensitive proportional counter. Fig. 4 shows X-ray spectra for the transitions from the  $n=3$  excited states to the ground state ( $2p^6$ ) in Ne-like ions of Ba ( $Z=56$ ), Cs(55), Xe(54), I(53), Te(52), Sb(51) and Sn(50) as a function of the scaled transition energy:  $E(\text{transition energy})/E_{av}(\text{configuration averaged energy})$ . In this figure, 3D, 3F and 3E denote some electronic configurations in the  $n=3$  excited states, which are  $(2p_{3/2}^{-1}3d_{5/2})_{J=1}$ ,  $(2p_{1/2}^{-1}3s)_{J=1}$  and  $(2p_{3/2}^{-1}3d_{3/2})_{J=1}$ , respectively. As seen in Fig. 4, the order of excited levels changes between 3D and 3F, and also between 3F and 3E. For example, the 3D and 3F lines become closer, change posi-

tions at  $Z = 54$  ( $\text{Xe}^{54+}$ ) and then become far again as  $Z$  increases. This means that in this  $Z$  region the energy levels of these states become degenerating, so that the wave functions of these states might mix strongly.

The experimental wavelengths are compared to the theoretical values calculated with the multi-configuration Dirac-Fock (MCDF) method. The experimental and the theoretical results of the transition energies for 3D, 3F and 3E lines are plotted in Fig. 5. Two types of calculations have been performed: 1) with configuration mixing of the wavefunctions and 2) without mixing, respectively. The calculated values with configuration mixing reproduce the experimental results quite well. As is shown in Fig. 5, both of the experimental and the theoretical investigations clearly indicate that the two levels get close to each other around  $Z = 55$  for 3D and 3F,  $Z = 51$  for 3F and 3E, but avoid degenerating. This suggests that they are coupled through strong mixing of two electronic configurations.

### Visible Spectroscopy

Forbidden transitions with long wavelengths sometimes play important roles in diagnostics of hot plasmas. In the visible region, the ion temperature and the local magnetic field could be easily determined through the measurements of Doppler and polarization profiles of emission lines from

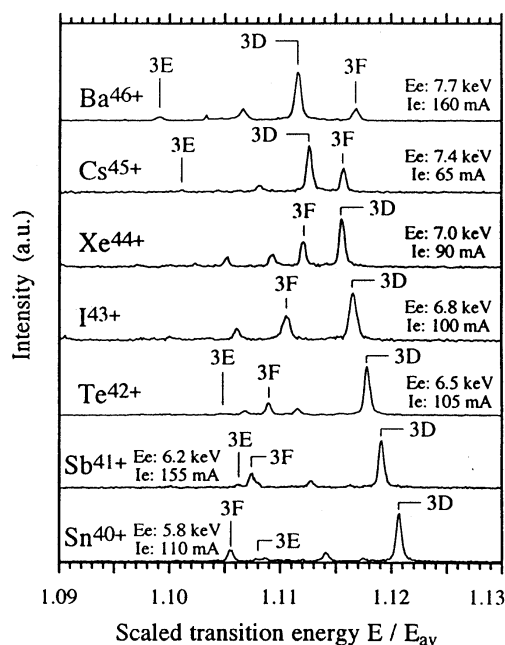


Fig. 4. X-ray spectra from Ne-like ions of various elements. The horizontal axis is the scaled X-ray energy:  $E(\text{transition energy})/E_{\text{av}}$  (configuration averaged energy in  $(2p^{-1}3l)$ ).

HClIs in a plasma.

At lower interaction energies of electrons with the trapped HClIs, we have systematically observed visible spectra due to fine structure M1 transitions,  $(3D^4)^5D_2-^5D_3$ , in the ground term of Ti-like ions for several elements with  $Z = 51-78$ .<sup>7</sup> The present observation has been made by using the 32-cm monochromator of Czerny-Turner type with a liquid nitrogen cooled CCD detector. The spectra obtained are shown in Fig. 6. In this figure, the target elements of Ti-like ions observed are given together with the atomic number  $Z$ , the electron beam parameter and the data acquisition time. From Sb ( $Z = 51$ ) to Pt (78), all of the M1 transitions,  $^5D_2-^5D_3$ , in the Ti-like ions exhibit anomalous wavelength independence of  $Z$ , lying in the visible or near UV region, which is qualitatively in agreement with the prediction by Feldman et al.<sup>10</sup>

This anomalous stability in the wavelength variation with  $Z$  has been discussed based on our theoretical calculation with the MCDF method. From consideration of mixing coefficients in the coupling scheme with respect to  $Z$ , the levels which are well described by the LS coupling scheme in low  $Z$  become characterized by the JJ coupling scheme in high  $Z$ . The transition from LS to JJ coupling takes place in the narrow intermediate region between  $Z = 40$  and 60. According to the calculation of the  $^5D_2-^5D_3$  transition energies, a plateau, that is, the anomalous wavelength-stability with  $Z$ , is formed accidentally due to the transition from LS to JJ coupling.

The present calculations for the transition energies are in excellent agreement with all the existing measurements reducing the discrepancy to less than 1% (Fig. 7). This suggests that the present calculation may well fill the void of unmea-

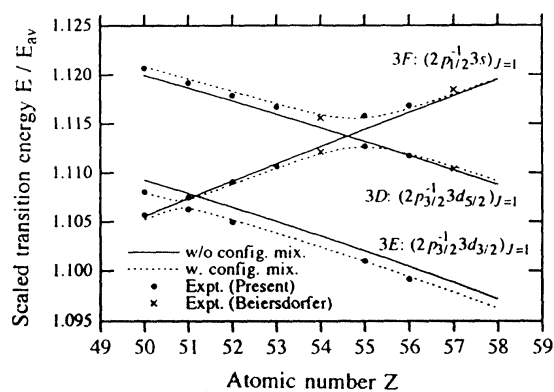


Fig. 5. Experimental and theoretical transition energies for 3D, 3F and 3E in the scaled unit as a function of the atomic number  $Z$ . Crosses represent the experimental values obtained by Beiersdorfer.<sup>6</sup>

sured elements from Sn ( $Z = 50$ ) to U ( $Z = 92$ ).

### HCI-surface Interactions

From a technical view point of the ion source, the EBIT has unique characteristics, such as low emittance, cold and very high charge-state ions, for a variety of applications in the research of ion-surface interactions.

Studies of reactions between slow, very HCIs and surfaces could be performed recently by using the EBITs. In principle, low-energy ions with very high charge-states are extracted from the EBIT. These ions have total potential energies in excess of over 100 keV, even if their kinetic energies

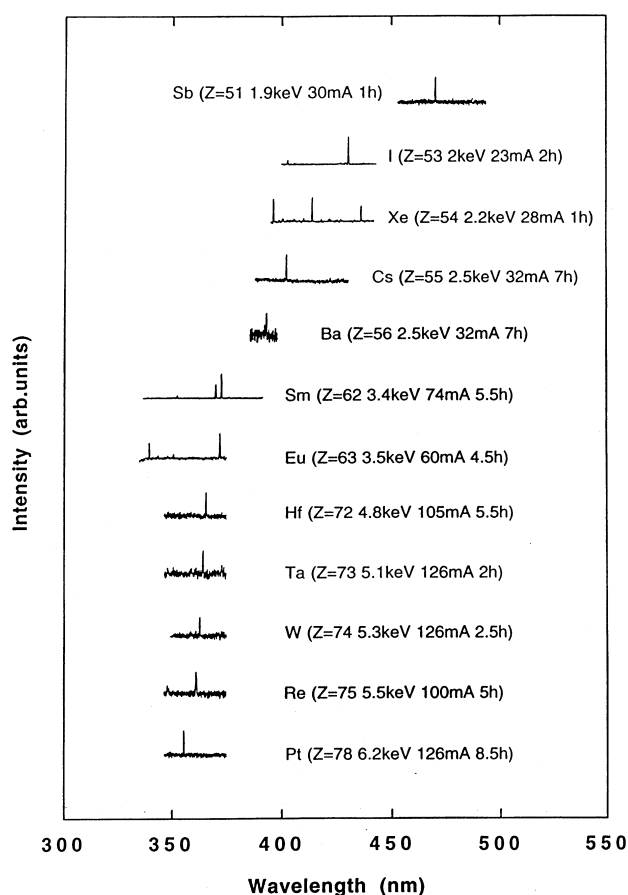


Fig. 6. Visible spectra from Ti-like ions of various high  $Z$  elements. The vertical scale of the individual spectrum is adjusted so that the heights of the lines are almost the same. The experimental conditions are also shown in the figure. In the spectrum for Xe ions, lines at around 396 nm and 436 nm are identified to be transitions in V- and Kr-like Xe ions, respectively. For Sm and Eu,  $(3d^4)^5D_4-^5D_3$  transitions are additionally observed.

are small. It is of fundamental interest to understand the mechanism of the energy deposition and how the large potential energy is lost and distributed to a variety of excitations during their interaction with a solid surface.

So far, there are a large number of experiments using the EBITs to study various fundamental processes such as electron-, other particle- and X-ray-emission, scattering, charge transfer and surface-defect formation. These studies are of wide-spread and long-standing interest from the viewpoint of both basic and applied physics.

In the Tokyo-EBIT facility, we have started to participate in the research field of the HCI-surface interactions. At the first stage, we have prepared various kinds of tools for surface physics experiments and made preliminary observations. In this report, we introduce just the microscopic study. The microscopic observations have been made to study the surface defects produced by slow HCI impact on a solid surface. The surface topography of the samples is investigated using a scanning tunneling microscope (STM). A typical example of the observations is shown in Fig. 8. In this figure, a STM image shows the defects formed on highly oriented pyrolytic graphite (HOPG) surface. A defect ( $1 \sim 3$  nm in diameter) is considered to be created by the impact of a single  $Kr^{33+}$  ion (500 V/q). The mechanism of defect formation by HCI impact are being investigated through various experiments using slow HCIs with different energies and charge-states impact on the insulator, semiconductor, metal surfaces.

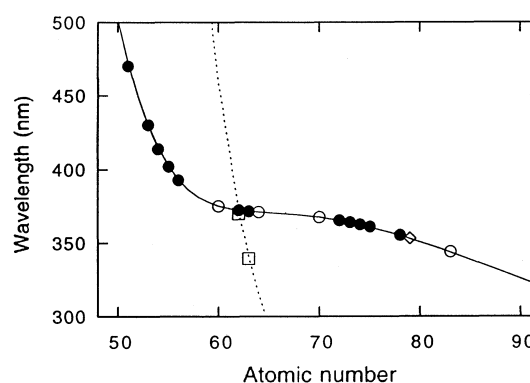


Fig. 7. Wavelengths of the  $(3d^4)^5D_2-^5D_3$  transition in Ti-like ions as a function of the atomic number. Solid circles are from the present measurements, open circles  $\circ$  from the NIST group,<sup>8</sup> and open diamonds  $\diamond$  from the LLNL group.<sup>9</sup> The solid line represents the present theoretical values. The results for the  $(3d^4)^5D_4-^5D_3$  transition are also shown, together with the theoretical values (dashed line).

## FUTURE PLANS

In addition to the research works described above, several kinds of activities are in progress on HCIs with the Tokyo-EBIT, such as the measurement of ionization cross sections for H- and He-like ions by electron impact, the observations of two-electron contribution to the 1s binding energies in He-like ions and some theoretical works. Constant efforts for machine study are also going on, for e.g. diagnostics of the electron beam using the Thomson scattering method, developments of novel cooling techniques for trapped HCIs and so on.

The present maximum energy of the electron beam achieved is 150 keV. We are making efforts to raise the beam energy, providing various protections from heavy discharging at the high voltage applications. The maximum beam current is presently 300 mA. As is seen in Fig. 9, independently of the beam energy, the emission current is determined by the potential difference between the cathode and the anode in the

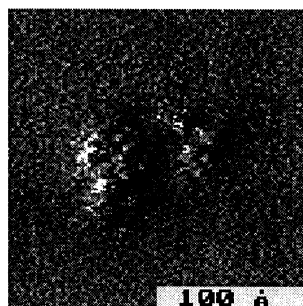


Fig. 8. A scanning tunneling microscope (STM) image showing the defects formed on a highly oriented pyrolytic graphite (HOPG) surface by slow (500 V/q)  $\text{Kr}^{33+}$  ion-impact.

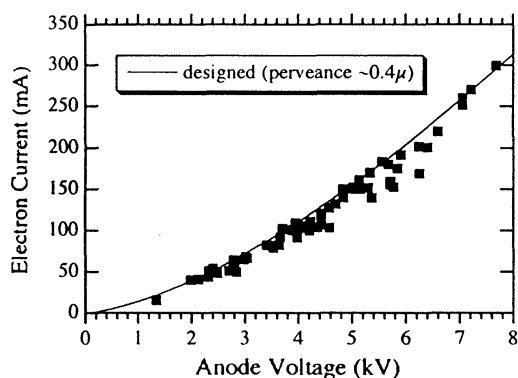


Fig. 9. Measured electron beam currents dependent on the anode voltage to the cathode potential. A solid line shows the designed value from the micro-perveance of  $0.4 \mu\text{A}/\text{V}^{3/2}$ .

electron gun, which was originally designed to generate the completely magnetized electron-flows.

In the high energy-electron beam operations, the following research subjects are being planned.

1. HCI-electron interactions
  - 1) high resolution study for DR processes, to see DR spectral line shapes, to see interference effects with RR,
  - 2) ionization cross sections of heavy HCIs, to see resonances, to measure e-energy dependences.
2. X-ray spectroscopy
  - 1) 1s Lamb shift by intercomparison method, to measure the wavelength difference between Ly-alpha of  $\text{In}^{48+}$  and Ly-beta of  $\text{Rh}^{44+}$ ,
  - 2) DR and/or other resonant processes.
3. Visible spectroscopy
  - 1) (hyper) fine structure of high Z ions.
4. Ion trap experiments
  - 1) cooling trapped HCIs, test of various techniques,
  - 2) laser spectroscopy,
  - 3) excitation of ion motions by RF *in situ*, to remove undesired ions from the trap.
5. HCI-surface interactions
  - 1) STM observations, nanofabrication, to see target (metal, in situ, ...) dependence,
  - 2) multiparameter coincidence for emitted particles/photons.
6. HCI-A/M (Cluster) interactions
  - 1) fragmentations, to see species of fragments, to measure HCI-internal energy conversions to translational energy of fragments,
  - 2) bio-chemical reactions of HCIs.
7. Nuclear processes in bare, H-like ions (Dy, Re, Os, Tl, Pb, ...), bound-state beta decay, nuclear excitation by electronic transition (NEET), ...

## ACKNOWLEDGMENTS

The research activity described above is being performed under the auspices of the International Co-Operative Research Project (ICORP) of the Japan Science and Technology Corporation (JST). The collaborative study is in progress with Prof. J. D. Silver of the University of Oxford on HCIs and also with Dr. H. A. Klein of the National Physical Laboratory on ion trap physics.

Finally, listed below are the names of JST colleagues

and also of collaborators from other institutions.

D. Kato, T. Kinugawa, H. Kuramoto, N. Nakamura, H. Shimizu, X-M. Tong, C. Yamada and H. Watanabe.

E. J. Sokell (Univ. College Dublin), F. J. Currell (Queens Univ. Belfast), T. Hirayama (Gakushuin Univ.), K. Motohashi (Tokyo Univ. Agric. Technol.), K. Okazaki (RIKEN), M. Sakurai (Kobe Univ.), S. Tsurubuchi (Tokyo Univ. Agric. Technol.), I. Yamada and T. Watanabe (Int. Christian Univ.).

A number of graduate students have been participating in this research project. The author is grateful to all of the above colleagues for their collaboration.

Received December 31, 2000.

### Key Words

Highly Charged Ion (HCI); Electron Beam Ion Trap (EBIT).

### REFERENCES

1. Levine, M. A.; Marrs, R. E.; Henderson, J. R.; Knapp, D. A.; Schneider, M. B. *Physica Scripta* **1998**, T22, 157.
2. Donets, E. D.; Orsyannikov, V. P. *Sov. Phys. JETP* **1981**, 53, 466.
3. Crespo López-Urrutia, J. R.; Bapat, B.; Dorn, A.; Moshhammer, R.; Ullrich, J. *Abstract of ICPEAC, Sendai* **1999**, 742.
4. Watanabe, H.; Asada, J.; Currell, F. J.; Fukami, T.; Hirayama, T.; Motohashi, K.; Nakamura, N.; Nojikawa, E.; Ohtani, S.; Okazaki, K.; Sakurai, M.; Shimizu, H.; Tada, N.; Tsurubuchi, S. *J. Phys. Soc. Jpn.* **1997**, 66, 3795.
5. Nakamura, N.; Kato, D.; Ohtani, S. *Phys. Rev.* **2000**, A61, 052510.
6. Beiersdorfer, P.; von Goeler, S.; Bitter, M.; Hinnov, E.; Bell, R.; Bernabei, S.; Felt, J.; Hill, K. W.; Hulse, R.; Stevens, J.; Suckewer, S.; Timberlake, J.; Wouster, A.; Chen, M. H.; Scofield, R. S.; Dietrich, D. D.; Gerassimenko, M.; Silver, E.; Walling, R. S.; Hagelstein, P. L. *Phys. Rev.* **1988**, A37, 4153.
7. Watanabe, H.; Crosby, D.; Currell, F. J.; Fukami, T.; Kato, D.; Ohtani, S.; Silver, J. D.; Yamada, C. *Phys. Rev.* **2001**, A63, 042513.
8. Serpa, F. G.; Meyer, E. S.; Morgan, C. A.; Gillaspay, J. D.; Sugar, J.; Roberts, J. R.; Brown, C. M.; Feldman, U. *Phys. Rev.* **1996**, A53, 2220; Porto, J. V.; Kink, I.; Gillaspay, J. D. *Phys. Rev.* **2000**, A61, 054501.
9. Träbert, E.; Beiersdorfer, P.; Urtter, Crespo López-Urrutia, J. R. *Physica Scripta* **1988**, 58, 599.
10. Feldman, U.; Indelicato, P.; Sugar, J. *J. Opt. Soc. Am.* **1991**, B8, 3.